

Magnetic Circular Dichroism and Absorption Spectra of Phosphinidene in Noble-Gas Matrices

Jeremy J. Harrison[†] and Bryce E. Williamson*

Department of Chemistry, University of Canterbury, Private Bag 4800, Christchurch, New Zealand

Received: October 13, 2004; In Final Form: November 14, 2004

Electronic magnetic circular dichroism and absorption spectra are reported for the $A^3\Pi_1 \leftarrow X^3\Sigma^-$ transitions of phosphinidene (PH) isolated in Ar, Kr, and Xe matrices at cryogenic temperatures (~ 1.4 – 20 K) and over a range of magnetic field strengths (0 – 5 T). The results are analyzed by the method of moments, and parameters are extracted by fitting the experimental data to a model in which the $A^3\Pi_1$ term is split by spin–orbit (SO) coupling interactions, while the $X^3\Sigma^-$ term is split by spin–spin and higher-order SO coupling. The analysis indicates that, unlike the equivalent imidogen (NH) systems, ground-state PH radicals isolated in noble-gas matrices do not behave as free rotors. Trends in excited-state SO coupling constants are attributed to the external heavy-atom effect and guest–host orbital mixing. It is tentatively concluded that librational amplitudes of the guest radical decrease in the order $Ar > Xe > Kr$, probably as a consequence of competition between stronger guest–host interactions and larger matrix sites in heavier hosts.

I. Introduction

We have previously published magnetic circular dichroism (MCD) and absorption spectra for the $A^3\Pi_1 \leftarrow X^3\Sigma^-$ transition of the imidogen (NH) radical isolated in Ar,¹ Kr, Xe, and N₂ matrices.² These data were analyzed to obtain excited-state spin–orbit (SO) coupling parameters, which were found to be compatible with an external heavy-atom effect due to the host atoms. For the noble-gas matrices (NH/NG; NG = Ar, Kr, and Xe), the ground-state guest radicals were found to act essentially as free rotors, in agreement with the conclusions of previous workers.^{3,4} However, for NH/N₂, rotation was significantly hindered, resulting in a significant zero-field splitting (ZFS) of $D' = 0.61 \pm 0.02$ cm⁻¹ in the $X^3\Sigma^-$ ground state.

Here we report MCD and absorption spectra for the closely related phosphinidene (PH)/NG systems with the aim of establishing trends that reflect guest–host interactions and the dynamics of the guest radical.⁵ (Attempts to measure the spectra of PH/N₂ were problematic because of the production of NH, whose strong, broad $A^3\Pi_1 \leftarrow X^3\Sigma^-$ absorption band overlapped the equivalent band of PH/N₂.)

Previous investigations of PH have been confined to the gas phase. In 1907, Geuter reported emission at 340 nm from a discharge in phosphorus and hydrogen.^{6,7} This was further investigated in the 1930s by Pearse, who assigned it to $^3\Pi_1 - ^3\Sigma^-$ of PH.^{6,8} Much later, Legay reported an analysis of the (1, 0) absorption band.⁹ Then in 1974, Rostas and co-workers published a detailed analysis of the emission spectra of PH and PD, deriving electronic and rotational parameters for the ground and excited states.¹⁰

The absorption and MCD results presented in this article are the first reported for PH radicals trapped in inert, solid matrices.

II. Experimental Section

Samples were prepared by a method similar to that described previously for NH/NG.² PH₃ (Matheson; ULSI 5N7 purity) was mixed with Ar (Matheson; UHP 99.999%), Kr (Linde; 99.99 vol %), or Xe (Linde; 99.99 vol %) to a pressure of ~ 1 atm at mole ratios of $\sim 1:100$. PH was produced by subjecting the mixture to a Tesla coil discharge as it flowed at ~ 2 – 3 mmol h⁻¹ through a 12-mm (i.d.) quartz tube. The products were deposited for 40–60 min onto a cryogenically cooled *c*-cut sapphire sample window held at a temperature below 20 K.

Preliminary experiments were performed using a He-refrigerator/electromagnet system, which permits temperatures down to ~ 12 K and magnetic fields up to ~ 0.6 T.^{11,12} More definitive results were obtained using a matrix-injection system comprising a 6-T Oxford Instruments SM4 magneto-cryostat, a matrix-deposition chamber, and a siphon rod, the tip of which contains a sapphire window.^{13,14} Temperatures above 4.2 K were monitored by using a calibrated carbon resistor, while lower temperatures, down to ~ 1.4 K, were obtained by pumping the vapor above the liquid and were determined by measuring the pressure¹⁵ with a capacitance manometer.

MCD (ΔA) and absorption (A) spectra were measured simultaneously using a double-beam spectrometer,^{11,12} operating under the conditions described for NH/NG.² ΔA is the difference between the absorbance of left and right circularly polarized light by a sample in the presence of a longitudinal magnetic field of inductance B , while A is the corresponding average absorbance.¹⁶

$$\Delta A = A_{\text{lcp}} - A_{\text{rcp}} \quad (1)$$

$$A = \frac{A_{\text{lcp}} + A_{\text{rcp}}}{2} \quad (2)$$

III. Results

Absorption spectra and the temperature dependence (at $B = 1$ T) of the MCD are shown for the (0, 0) bands of the $A^3\Pi_1 \leftarrow$

* Corresponding author. E-mail: bryce.williamson@canterbury.ac.nz. Fax: ++ 64 3 364 2110. Tel.: ++ 64 3 364 2439.

[†] Present address: The Department of Chemistry, University of Oxford, The Physical and Theoretical Chemistry Laboratory, South Parks Road, Oxford, OX1 3QZ, United Kingdom.

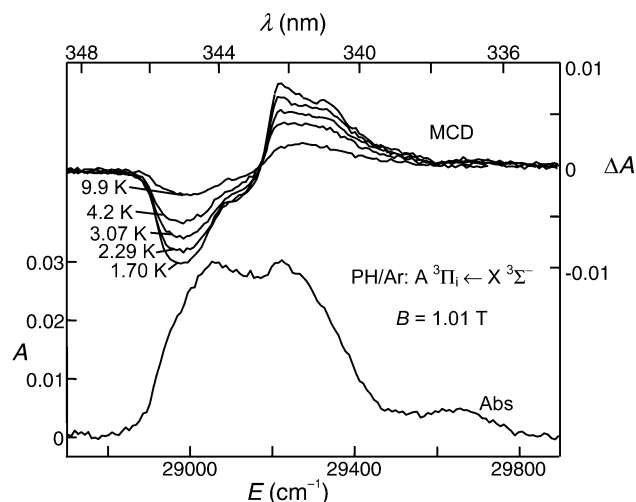


Figure 1. Absorption (bottom) and temperature-dependent MCD spectra (1.01 T) of the (0, 0) band of the $A^3\Pi_i \leftarrow X^3\Sigma^-$ transition of PH/Ar.

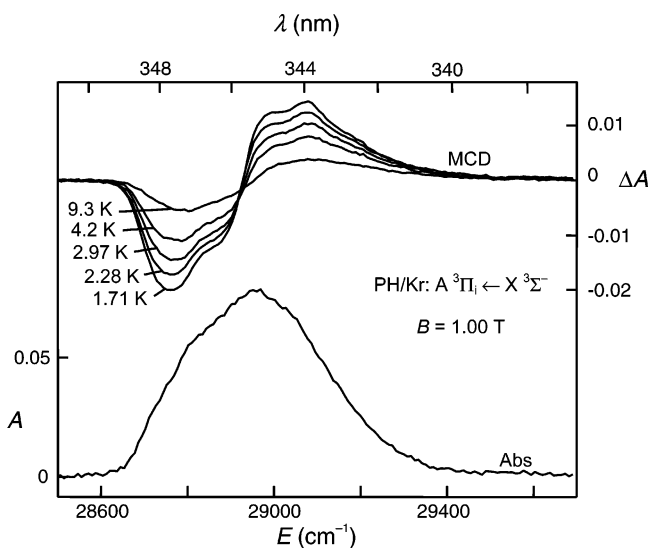


Figure 2. Absorption (bottom) and temperature-dependent MCD spectra (1.00 T) of the (0, 0) band of the $A^3\Pi_i \leftarrow X^3\Sigma^-$ transition of PH/Kr.

$X^3\Sigma^-$ transitions of PH/NG in Figures 1–3. All of the MCD spectra have the double-signed dispersion observed for $A^3\Pi_i \leftarrow X^3\Sigma^-$ of NH/NG,^{1,2,17,18} which is normally taken to indicate the presence of \mathcal{A} terms.¹⁶ However, they also exhibit temperature dependence and magnetization saturation (shown for PH/Xe in Figure 4), which are indicative of \mathcal{C} terms.¹⁶ Very weak temperature and magnetic-field dependences of the absorption spectra at the lowest temperatures suggest the presence of levels within the manifold of the $X^3\Sigma^-$ term whose energy separations are of a magnitude similar to their Zeeman shifts.

The spectra were quantified by using moment analysis.¹⁶ The n th absorbance and MCD moments are, respectively,

$$\mathbf{A}_n = \int_{\text{band}} \frac{A(E)}{E} (E - \bar{E})^n dE \quad (3)$$

$$\mathbf{M}_n = \int_{\text{band}} \frac{\Delta A(E)}{E} (E - \bar{E})^n dE \quad (4)$$

Here, E is the photon energy, \bar{E} is the absorption band barycenter (the average energy defined by the requirement that $\mathbf{A}_1 = 0$),

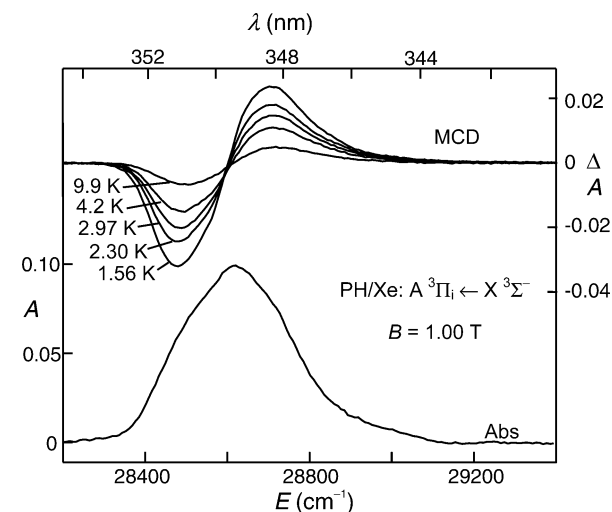


Figure 3. Absorption (bottom) and temperature-dependent MCD spectra (1.01 T) of the (0, 0) band of the $A^3\Pi_i \leftarrow X^3\Sigma^-$ transition of PH/Xe.

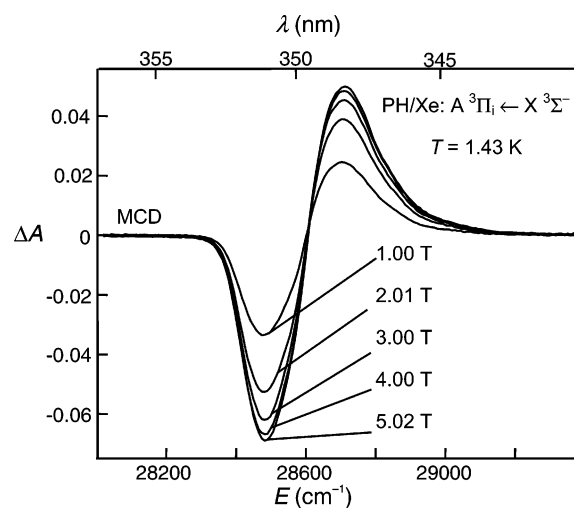


Figure 4. Magnetic-field dependence of the MCD spectrum (1.43 K) of the (0, 0) band of the $A^3\Pi_i \leftarrow X^3\Sigma^-$ transition of PH/Xe.

TABLE 1: Parameters (cm^{-1}) for the $A^3\Pi_i \leftarrow X^3\Sigma^-$ Transition of PH in the Gas Phase and in Noble-Gas Matrices

	\bar{E}	$2(\mathbf{A}_2/\mathbf{A}_0)^{1/2}$	$\Delta G'_{1/2}$	A_{Π}	D'
PH(gas)			1833.8 ^{9,10}	-115.7 ^{10,20}	<i>a</i>
PH/Ar	29 190 ± 20	350 ± 10	1825 ± 10	-192 ± 3	1.62 ± 0.07
PH/Kr	28 980 ± 20	360 ± 10	1795 ± 10	-133 ± 3	1.40 ± 0.10
PH/Xe	28 640 ± 20	270 ± 10	1760 ± 10	-107 ± 1	0.73 ± 0.04

^a The gas-phase value of D is 4.42 cm^{-1} .^{10,20}

and the integrals are evaluated numerically over the full envelope of the (0, 0) transition.

The (0, 0) band barycenters and associated effective bandwidth parameters, $2(\mathbf{A}_2/\mathbf{A}_0)^{1/2}$, are collected in Table 1. In agreement with observations for NH_2 and other molecules trapped in noble-gas matrices,¹⁹ there is a bathochromic shift with increasing atomic number of the noble-gas host. The bands are two or three times broader than those for NH/NG but only about half as broad as for NH/ N_2 .

The $\mathbf{M}_1/\mathbf{A}_0$ ratios are plotted for various magnetic-field strengths against $1/kT$ ($k = 0.695 \text{ cm}^{-1} \text{ K}^{-1}$ is Boltzmann's constant) in Figures 5–7. These plots clearly exhibit the saturation behavior with decreasing temperature and increasing magnetic field that is characteristic of \mathcal{C} terms.

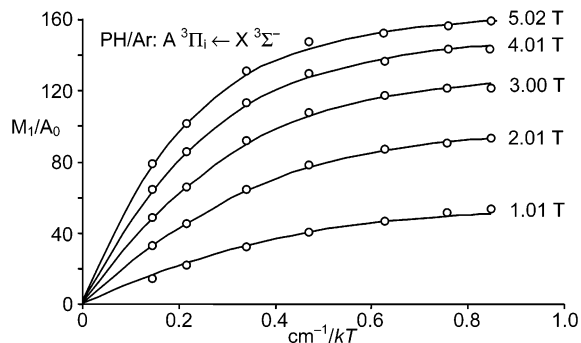


Figure 5. Temperature dependence of the moment ratio M_1/A_0 as a function of $1/kT$ for the (0, 0) band of the $A^3\Pi_i \leftarrow X^3\Sigma^-$ transition of PH/Ar. The curves are the best fits to all data using eq 5 with $A_\Pi = -192 \text{ cm}^{-1}$ and $D' = 1.62 \text{ cm}^{-1}$.

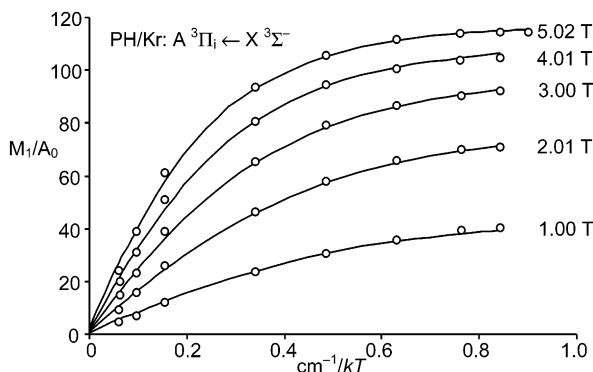


Figure 6. Temperature dependence of the moment ratio M_1/A_0 as a function of $1/kT$ for the (0, 0) band of the $A^3\Pi_i \leftarrow X^3\Sigma^-$ transition of PH/Kr. The curves are the best fits to all data using eq 5 with $A_\Pi = -133 \text{ cm}^{-1}$ and $D' = 1.40 \text{ cm}^{-1}$.

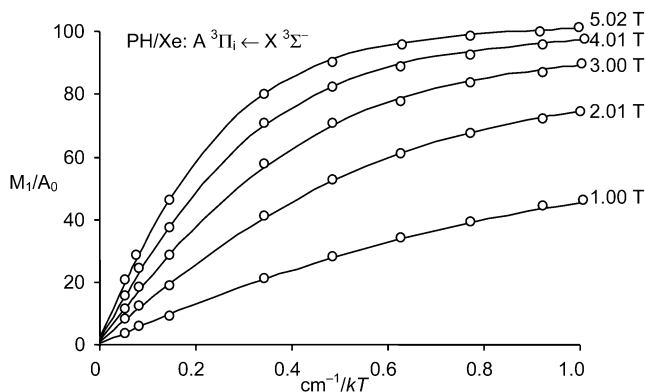


Figure 7. Temperature dependence of the moment ratio M_1/A_0 as a function of $1/kT$ for the (0, 0) band of the $A^3\Pi_i \leftarrow X^3\Sigma^-$ transition of PH/Xe. The curves are the best fits to all data using eq 5 with $A_\Pi = -107 \text{ cm}^{-1}$ and $D' = 0.73 \text{ cm}^{-1}$.

Spectra of the (1, 0) band also were measured using the He-refrigerator/electromagnet system. The values of $\Delta G'_{1/2}$, given in Table 1, show a slight decrease (relative to the gas phase) on incorporation into an Ar matrix, with further decreases for heavier hosts.

IV. Discussion

The $A^3\Pi_i \leftarrow X^3\Sigma^-$ transitions for PH arise from $2\pi \leftarrow 5\sigma$ excitations where the 2π orbitals are nonbonding $3p_{\pm 1}$ orbitals of the P atom and the 5σ is an admixture, mainly of $3p_0$ with the H(1s) orbital. These transitions are closely analogous to those with the same designation for NH, and their analysis is essentially the same as that which we have described earlier.^{1,2}

The most significant alteration is the omission of consideration of excited-state crystal-field effects. Although these will certainly be present for PH/NG, they do not affect the lower spectroscopic moments,¹⁶ and the spectra do not exhibit sufficient structural detail to permit the more explicit modeling of the band shapes that is required for their elucidation.¹

The excited states, designated $|\Sigma^3\Pi_{|\Omega|} \Lambda \Sigma\rangle$ in a Hund's case (a) basis, are split by first-order SO coupling into three levels according to the value of $|\Omega|$. In the gas phase, the SO coupling constant is $A_\Pi = -115.7 \text{ cm}^{-1}$,^{10,20} but its value can be substantially modified by incorporation of the radical into a condensed phase. Spin-spin (SS) and higher-order SO coupling slightly modify the separations and produce a small splitting of the $^3\Pi_{0\pm}$ level, but the relevant parameters are 2 orders of magnitude weaker than A_Π ,^{10,20} and their effects are neglected in this analysis.

It is also convenient to use a Hund's case (a) basis for the $X^3\Sigma^-$ term, with the states being designated as $|\Sigma^3\Sigma^- \Sigma\rangle$, where $\Lambda = 0$ and $\Omega = \Sigma = 0, \pm 1$. There is no first-order SO effect, but SS and higher-order SO coupling (mainly involving the $b^1\Sigma^+$ state) cause a ZFS, which, for the gas-phase radical, is measured by the parameter $D = 4.42 \text{ cm}^{-1}$.^{10,20} This value is 2.6 times larger than that for the $X^3\Sigma^-$ term of NH,²¹ the smaller SS contribution (arising from the more diffuse orbitals) being more than offset by a substantially larger SO contribution.^{20,22} For a $^3\Sigma^-$ free rotor in the absence of an external magnetic field, the lowest ($J = 1$) rotational level is necessarily threefold degenerate. However, when rotation is hindered, the electronic angular momenta couple to the internuclear axis and the $J = 1$ level develops a ZFS, denoted by the effective parameter D' , with the $|\Sigma^3\Sigma^- \pm 1\rangle$ states lying higher than $|\Sigma^3\Sigma^- 0\rangle$.

The MCD and absorption moments provide a means by which to evaluate the parameters A_Π and D' and, hence, to investigate guest-host interactions and the dynamics of the guest. The theoretical basis for this approach has been presented previously;¹ the crucial relationship is

$$M_1/A_0 = \mu_B B + (3A_\Pi/2) \int_{-1}^1 \sum_{i=1}^3 P_i (|C_{+i,j}|^2 - |C_{-i,j}|^2) \cos \theta \, d \cos \theta \quad (5)$$

where θ is the angle between the magnetic-field direction and the internuclear axis of the radical. The first term, $\mu_B B$, is the \mathcal{A} -term contribution from the orbital angular momentum of the excited state. The second, integral, term corresponds to oppositely signed \mathcal{C} terms of equal intensity that are separated by excited-state SO coupling and, hence, the dependence on A_Π . The $C_{\Sigma,i}$ are magnetic-field and orientation dependent coefficients that relate the case (a) basis functions of $X^3\Sigma^-$ to the eigenfunctions of the effective Hamiltonian in eq 6.

$$\mathcal{H} = g_e \mu_B B (S_z \cos \theta + S_x \sin \theta) + D' (S_z^2 - 2/3) \quad (6)$$

The nonlinear dependences on temperature and magnetic-field strength enter through the Boltzmann populations, P_i , in eq 5.

Accurate fits of eq 5 to the experimental M_1/A_0 data are obtained using the A_Π and D' parameters listed in Table 1 and are superimposed on the experimental data in Figures 5–7. The nonzero intercepts of the fits are a consequence of the \mathcal{A} terms, while the curvature is due to the \mathcal{C} terms. Consistent with the observation of very weak temperature and magnetic-field dependences of the absorption, the values of D' are similar to the Zeeman shifts, which are $\approx 2.3 \text{ cm}^{-1}$ ($g_e \mu_B B$) for randomly oriented $^3\Sigma$ systems in magnetic fields of $B \leq 5 \text{ T}$.

TABLE 2: One-Electron SO Coupling Constants (cm^{-1}) for the ^2P Terms of Metals and A $^3\Pi_i$ Terms of NH and PH in the Gas Phase and in Noble-Gas Matrices

guest species	ζ_p								a_π	
	Li ^{24,25}	Na ²⁴	K ²⁶	Ca ²⁶	Cu ²⁷	Ag ²⁸	Au ²⁸	NH ²	PH	
gas phase	0.23	11.5	38.5	369	166	614	2543	34.8	115.7	
Ar	-16				124	783	3354	33.5	192	
Kr	-70		-64		95	638	3110	21	133	
Xe	-196	-213	-170	100-150	-23	583	2655	25.6	107	

In Table 2, the one-electron SO coupling constants ($a_\pi = |A_{\Pi}|$) for PH/NG and NH/NG are compared with equivalent parameters (ζ_p) for the ^2P terms of some alkali and coinage metals. As noted previously,² the behavior of a_π for NH/NG, a slight decrease on incorporation into Ar, followed by further diminution for heavier hosts, parallels that for lighter metal systems such as Cu/NG. In comparison, the trends for PH/NG are more consistent with heavier metal systems such as Ag/NG and Au/NG, a larger value of a_π in Ar, followed by a monotonic decrease to Xe. The similar behavior for the metal atoms and diatomic radicals points to a common, external heavy-atom effect,²³ which increases rapidly as the atomic number of the host becomes larger.

As noted above, rotational hindrance gives rise to a nonzero D' , which can, in principle, approach the gas-phase D value. Near-zero D' values found for NH/NG (compared with $D = 1.67 \text{ cm}^{-1}$ for gas-phase NH)²¹ were, therefore, interpreted^{1,2} as corroboration of conclusions by earlier workers using other techniques^{3,4} that ground-state NH behaves as a free rotor in noble-gas matrices. In contrast, $D' = 0.61 \text{ cm}^{-1}$ for NH/N₂² is consistent with the expectation that guest rotations should be significantly hindered in nitrogen matrices.²⁹

The D' values for PH/NG (Table 1) are significantly nonzero, indicating that rotation of PH in noble-gas matrices is restricted in the ground state. However, they are still substantially quenched in comparison with the potential maximum ($\sim 4.42 \text{ cm}^{-1}$), with the ratio D'/D decreasing monotonically from ~ 0.37 (close to that for NH/N₂) in Ar to ~ 0.32 in Kr and ~ 0.17 in Xe. A simple interpretation of these results would be that the librational zero-point amplitude of the restricted rotor increases with the atomic number of the host species, possibly as a consequence of larger matrix sites. But other evidence conflicts with such a conclusion. In particular, the systematic decrease of $\Delta G'_{1/2}$ in matrices of heavier gases (Table 1) points to increasing guest–host interactions, which (in accord with conventional chemical expectations) is likely to be related to guest–host orbital mixing. In the absence of other effects, this would lead to *greater* rotational hindrance and, hence, *larger* values of D' in the heavier matrices.

A more likely explanation for the decrease in D' lies with changes to the “magnetic” interactions. In the case of PH, the major contribution to D arises from higher-order SO coupling and can be expressed (to the second order in perturbation theory) as

$$D_{\text{SO}} = \frac{4a_\pi^2}{E(\text{b } ^1\Sigma^+) - E(\text{X } ^3\Sigma^-)} \quad (7)$$

Because a_π decreases with the atomic number of the host (Table 2), eq 7 indicates that D' might also be expected to decrease, in qualitative agreement with the observations. In addition, delocalization of electron density consequent on guest–host orbital mixing will lower the SS contribution, leading to further reduction of D' . When rotational dynamics are ignored, and assuming that the denominator in eq 7 does not change

significantly between the three matrices, these considerations suggest that the ratio D'/a_π^2 should diminish slightly with increasing atomic number of the host. In fact, the ratio increases significantly from $(4.4 \pm 0.2) \times 10^{-5} \text{ cm}$ for Ar to $(7.9 \pm 0.7) \times 10^{-5} \text{ cm}$ for Kr before decreasing to $(6.4 \pm 0.4) \times 10^{-5} \text{ cm}$ for Xe. These values are all significantly lower than the gas-phase value of $D/a_\pi^2 \approx 3.3 \times 10^{-4} \text{ cm}$, and they are interpreted to indicate that rotational hindrance increases in the order Ar < Xe < Kr, possibly due to an interplay between the strength of guest–host interactions and the size of the matrix sites occupied by the guests.

In earlier work on matrix-isolated NH,^{2,5} we observed a qualitative correlation between the breadth of the A $^3\Pi_i \leftarrow \text{X } ^3\Sigma^- (0, 0)$ band and the degree of rotational hindrance in the ground state, with the hindered NH/N₂ system having a bandwidth nearly four times greater than those for the (essentially) free-rotor NH/NG systems. The increase probably arises from a combination of excited-state crystal-field effects and inhomogeneity resulting from relaxation of the host lattice when the guest radical assumes a particular orientation in the host cavity. In the case of PH/NG, the significant decrease in the (0, 0) bandwidths from Kr to Xe (Table 1) lends support to the view that PH is more hindered in Kr. However, the same arguments would suggest that, on the basis of similar bandwidths, the degrees of hindrance in Ar and Kr should be similar, which contradicts the more compelling evidence from the trends of D' . This situation would be clarified by appropriate quantum-mechanical calculations. Further, the results reported here would be usefully augmented by measurements on PD/NG systems, which should provide additional information on ground-state motional effects via isotopic effects on D' .³⁰

V. Conclusions

This paper presents the first reported spectra for A $^3\Pi_i \leftarrow \text{X } ^3\Sigma^-$ of PH doped in noble-gas matrices. Moment analysis of the data has provided information concerning excited-state SO splittings and ground-state ZFSs, and their variations with the nature of the host lattice.

Incorporation of PH into an Ar matrix increases a_π , the one-electron SO coupling constant for the 2π highest occupied molecular orbital, by $\sim 66\%$ compared with the gas phase. A monotonic decrease then ensues to a value slightly lower than that for the gas phase in Xe. This behavior is analogous to that observed for other systems, suggesting that the same external heavy-atom mechanisms are responsible.

Unlike NH/NG, the values of D' (the ZFS of the lowest-energy levels of the ground state) for PH/NG are significantly nonzero, which indicates that rotation of the guest radical in its ground state is substantially hindered in all of the matrices examined. In Ar, D' is $\sim 36\%$ of the gas-phase value of D , decreasing to $\sim 17\%$ in Xe. This can be explained mainly as a secondary SO effect via interactions with the heavy atoms of the matrix.

Comparison of the trends of D' and a_π^2 suggests that the librational amplitudes of the ground-state hindered rotor increase with the host in the order Kr < Xe < Ar. However, further information is required to unambiguously interpret the experimental data. The results and analyses for PH/NG⁵ and NH/NG^{1,2} would be usefully complemented by quantum calculations aimed at elucidating the details of the guest–host interactions and how they impinge on SO coupling and the guest dynamics. Experiments on PD/NG systems should also provide valuable information on motional effects.

Acknowledgment. We thank the University of Canterbury for providing J.J.H. with a Doctoral Scholarship.

References and Notes

- (1) Langford, V. S.; Williamson, B. E. *J. Phys. Chem. A* **1998**, *102*, 2415–2423.
- (2) Harrison, J. J.; Williamson, B. E.; Rose, J. L. *J. Phys. Chem. A* **2004**, *108*, 2633–2637.
- (3) McCarty, M. J.; Robinson, G. W. *J. Am. Chem. Soc.* **1959**, *81*, 4472–4476.
- (4) Bondybey, V. E.; Brus, L. E. *J. Chem. Phys.* **1975**, *63*, 794–804.
- (5) Harrison, J. J. PhD Thesis, University of Canterbury, Christchurch, 2003.
- (6) Pearse, R. W. B. *Proc. R. Soc. London, Ser. A* **1930**, *129*, 328–354.
- (7) Geuter, P. *Zeits. f. Wiss. Phot.* **1907**, *5*, 33–60.
- (8) Pearse, R. W. B.; Ishaque, M. I. *Proc. R. Soc. London, Ser. A* **1939**, *173*, 265–277.
- (9) Legay, F. *Can. J. Phys.* **1960**, *38*, 797–805.
- (10) Rostas, J.; Cossart, D.; Bastien, J. R. *Can. J. Phys.* **1974**, *52*, 1274–1287.
- (11) Langford, V. S.; Williamson, B. E. *J. Phys. Chem. A* **1997**, *101*, 3119–3124.
- (12) Langford, V. S. PhD Thesis, University of Canterbury, Christchurch, 1997.
- (13) Dunford, C. L. PhD Thesis, University of Canterbury, Christchurch, 1997.
- (14) Dunford, C. L.; Williamson, B. E. *J. Phys. Chem. A* **1997**, *101*, 2050–2054.
- (15) Durieux, M.; Rusby, R. L. *Metrologia* **1983**, *19*, 67–72.
- (16) Piepho, S. B.; Schatz, P. N. *Group Theory in Spectroscopy with Applications to Magnetic Circular Dichroism*; Wiley-Interscience: New York, 1983.
- (17) Rose, J. L. PhD Thesis, University of Virginia, Charlottesville, 1987.
- (18) Lund, P. A.; Hasan, Z.; Schatz, P. N.; Miller, J. H.; Andrews, L. *Chem. Phys. Lett.* **1982**, *91*, 437–439.
- (19) Meyer, B. *Low Temperature Spectroscopy*; American Elsevier Publishing Company: New York, 1971.
- (20) Horani, M.; Rostas, J.; Lefebvre-Brion, H. *Can. J. Phys.* **1967**, *45*, 3319–3331.
- (21) Veseth, L. *J. Phys. B: At. Mol. Phys.* **1972**, *5*, 229–241.
- (22) Wayne, F. D.; Colbourn, E. A. *Mol. Phys.* **1977**, *34*, 1141–1155.
- (23) Pellow, R.; Vala, M. *J. Chem. Phys.* **1989**, *90*, 5612–5621.
- (24) Rose, J.; Smith, D.; Williamson, B. E.; Schatz, P. N.; O'Brien, M. C. *M. J. Phys. Chem.* **1986**, *90*, 2608–2615.
- (25) Lund, P. A.; Smith, D.; Jacobs, S. M.; Schatz, P. N. *J. Phys. Chem.* **1984**, *88*, 31–42.
- (26) Samet, C.; Rose, J. L.; Schatz, P. N.; O'Brien, M. C. *M. Chem. Phys. Lett.* **1989**, *159*, 567–572.
- (27) Vala, M.; Zeringue, K.; ShakhEmampour, J.; Rivoal, J.-C.; Pyzalski, R. *J. Chem. Phys.* **1984**, *80*, 2401–2406.
- (28) Roser, D.; Pellow, R.; Eyring, M.; Vala, M.; Lignieres, J.; Rivoal, J.-C. *Chem. Phys.* **1992**, *166*, 393–409.
- (29) Durig, J. R.; Sullivan, J. F. In *Matrix Isolation Spectroscopy*, 1st ed.; Barnes, A. J., Orville-Thomas, W. J., Muller, A., Gaufres, R., Eds.; D. Reidel Publishing Company: Dordrecht, The Netherlands, 1981; pp 397–414.
- (30) Weltner, W. J. *Magnetic Atoms and Molecules*; Dover Publications: Mineola, 1989.